PHYSICAL REVIEW E **109**, 014702 (2024)

Dynamics of viscous droplet coalescence in the confined geometry of optical cells

P. V. Dolganov,* N. A. Spiridenko, and A. S. Zverev
Osipyan Institute of Solid State Physics RAS, 142432 Chernogolovka, Moscow Region, Russia

(Received 13 July 2023; accepted 28 December 2023; published 26 January 2024)

The dynamics of quasi-two-dimensional coalescence of isotropic droplets in nematic liquid crystal environment was studied. Investigations were made in confined geometry of a Hele-Shaw optical cell with different transverse droplet sizes. The existence of three distinct dynamic regimes was found for coalescence, namely, short-, middle-, and long-time regimes. The fast dynamics of bridge transformation was visualized. At short time the dynamics of droplet transformation is similar to the transformation of free (three-dimensional) droplets. At later stages, two regimes of the coalescence at different timescales are determined by Poiseuille flow. Experimental data are discussed on the basis of existing theories.

DOI: 10.1103/PhysRevE.109.014702

I. INTRODUCTION

Droplet coalescence is one of the most actively investigated areas of fluid dynamics [1–15]. Coalescence of liquid droplets is observed in everyday life, has wide technical applications, and for many years has been investigated experimentally and theoretically. It is relevant to different areas of science such as physics, chemistry, and biology. Theoretical studies of droplet coalescence are performed using different methods from scaling analysis to analytical and numerical calculations [16–23]. In recent decades high-speed cameras and electric methods are used in experiments that allow investigating processes previously unavailable for observation. The advantage of optical studies with temporal resolution up to about 10^{-4} s is the possibility to visualize the shape of a droplet during coalescence. The electric methods allow monitoring coalescence processes with resolution up to 10^{-8} s [3,4,24,25]; however, in these experiments the transformation of droplet form at coalescence can only be reconstructed on the basis of indirect data. The driving force of coalescence is surface energy or linear tension of the domain boundary. The nature of resistance can differ (can be related to viscosity μ or to inertia) which leads to complicated mechanisms of coalescence in systems with different materials, dimensions, and geometry. The majority of investigations so far were performed on three-dimensional droplets situated in air or in other liquids. The main attention in experimental investigations and theoretical calculations was paid to temporal transformation of the bridge region formed between two droplets at the initial stage of coalescence. Several regimes of bridge transformation were found for liquid droplets depending on viscosity of droplets and environment material: viscous, inertially limited viscous, and inertial regimes [4,24,25]. A more interesting situation is realized when the regime of bridge transformation changes during coalescence [3,4,24].

In recent years substantial attention was given to droplet coalescence in systems with reduced dimensionality. In particular, freestanding smectic films [26] are suitable media for modeling two-dimensional geometry. These films consist of a stack of parallel molecular layers. The thickness of the films is significantly smaller than their transverse size. Coalescence of islands (areas of larger thickness than the film), holes (areas of smaller thickness than the film), or isotropic droplets on smectic film are examples of quasi-two-dimensional coalescence [7–15]. Another example of quasi-two-dimensional behavior is the coalescence of two droplets in the confined geometry of a flat optical cell when the transverse size of droplets is larger than the cell thickness [27–29] or the coalescence of quasi-two-dimensional droplets with a bath of the same liquid [30–33]. In thin cells coalescence dynamics is strongly affected by Poiseuille flow with a large gradient of fluid velocity across the cell [30]. However, until recently quasi-two-dimensional droplet coalescence was investigated only on the latest state of the process when droplet shape relaxes to circular [27]. Recently it was found that the dynamics of large nematic droplets on the middle and late stages of coalescence is described by different laws [28].

In this paper, we present detailed experimental investigations of dynamic droplet evolution at coalescence in the confined geometry of a thin optical cell (here also referred to as the Hele-Shaw cell). Investigations were made on isotropic droplets in a nematic environment. Different regimes of coalescence were found with different functional temporal dependence of the size of the bridge connecting the two droplets. Three sequential (following one after the other) regimes and a crossover between them were not investigated previously in the same coalescence event both in quasi-two-dimensional and in three-dimensional coalescence. We used droplets with different sizes, which allows tracking the establishment and duration of the middle-time coalescence regime. Characteristic times of different stages of processes and their dependence on droplet size were determined. Experimental results are compared with existing theories.

II. EXPERIMENT

In our experiments we used nematic liquid crystal E7 (Synthon Chemicals). The material parameters of E7 can be found elsewhere [34–36]. The nematic liquid crystal was confined

---

*pauldol@issp.ac.ru

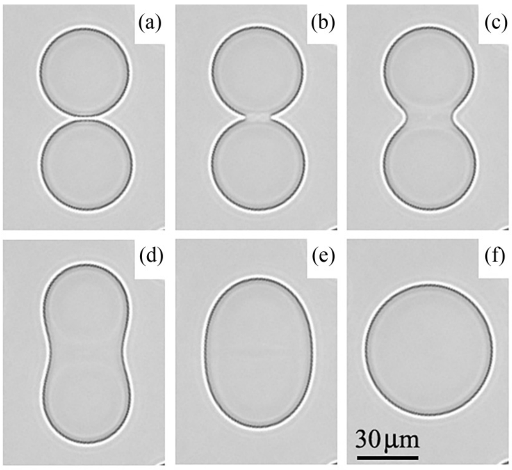

FIG. 1. A snapshot sequence of transformation of the droplet shape at coalescence. Isotropic droplets are located in a homeotropic nematic sample. Thickness of the cell is 19 µm. Droplet radii R are 21.8 and 22.5 µm. Times after the start of coalescence are 0.016 s (b), 0.05 s (c), 0.34 s (d), 3 s (e), and 16 s (f).

in a cell between two glass plates. Cells with homeotropic anchoring on the surfaces and with thickness ranging from 5 to 19 µm were used. The cell with the liquid crystal was deposited in a temperature-controlled stage (Mettler Toledo FP95 or Linkam LTS100) mounted on the table of an Olympus BX51 optical microscope. Isotropic droplets nucleated in nematic liquid crystal on heating near the nematic-isotropic transition and increased in size. During heating the sample was monitored visually. Then as the droplets reached necessary size, heating was stopped. We selected a pair of closely located droplets with approximately the same size without other droplets in their vicinity. To induce droplet coalescence, the sample was slowly heated with a typical velocity of 0.05 °C/ min so that the droplets grow and come into contact. The dynamics of the droplet shape during coalescence was directly recorded using optical microscopy with high-speed video cameras (Baumer VCXU-2C and Optronis Sprinter). Frame rates up to 1000 fps were used. Our measurements cover four decades of time.

III. RESULTS

Figure 1 shows a series of images illustrating the coalescence of two isotropic droplets of approximately equal size ($R \approx 21.8\,\mu\text{m}$ and $R \approx 22.5\,\mu\text{m}$) in a homeotropic nematic sample. Three distinct droplet shapes at different coalescence stages can be specified: two nearly circular droplets with a small bridge between them (b), waist-type (figure of eight) droplet (c), (d), and ellipsoidal droplet (e) relaxing into a circle (f). The duration of the relaxation stage is more than an order of magnitude larger than the range of existence of a waist-type droplet. Figure 2 shows schematically the starting stage of coalescence. R is the radius of the droplets. The contact region, which, as a rule, is called the bridge region, is highlighted by a dashed line and is shown in the right part of the figure. In many experimental and theoretical works the bridge width W was used as a quantitative characteristic of the coalescence dynamics. At long times, when the droplet shape becomes convex, the bridge width W is transformed to the minor axis of the ellipsoidal droplet.

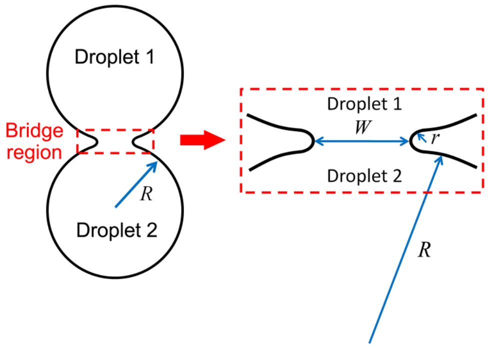

FIG. 2. A schematic of two equal droplets at the early stage of their coalescence (left) and bridge region between the droplets (right). R, W, and r are droplet radius, bridge width, and curvature radius at the edge of the bridge, respectively.

Figure 3(a) shows the temporal dependence of bridge width $W(t)$ for droplets of different initial radii R of about 22.5, 14.6, and 13.4 µm in the cell with gap $h = 5.5\,\mu\text{m}$. The velocity of the bridge expansion decreases with time. This behavior correlates with an intuitive consideration. At first, the main transformation takes place in a small region near the point of contact, while at the final stage, the material of the whole droplet relaxes to a circular form that decreases the flow velocity. The variation of geometrical characteristics on time at coalescence often follows the power law t^{β}. To understand more clearly the mechanism of coalescence, we present in Fig. 3(b) the log-log dependence of $W(t)$. In such presentation we can check the existence of coalescence regimes with power-law dependences $W(t)$ on time $W(t) = A(t - t_0)^{\beta}$. Clearly visible [Fig. 3(b)] are two nearly linear dependences in the log-log scale with a crossover between them. At short time $\beta \approx 1$, later a slower regime was observed. In the 5.5 µm cell the power at the middle stage is found to be $\beta \approx 1/4$ [Fig. 3(b)]. A similar dependence was observed in the inverse process at the coalescence of nematic droplets in an isotropic environment in thin cells [28]. At long times the functional dependence $W(t)$ is not clear from Fig. 3(b). The droplet shape at this stage is close to ellipsoidal. Deviation of the ellipse from a circular form can be described by the so-called shape factor $D(t) = [L(t)/W(t) - 1]$, where $L(t)/W(t)$ is the aspect ratio, and $L(t)$ and $W(t)$ denote the major and minor axes of the ellipse [27,37]. The log-time plot of $D(t)$ is given in Fig. 3(c). We see that $\ln D(t)$ decreases in a linear manner with time, which indicates exponential relaxation to circular form at the latest state of coalescence [Fig. 3(c)]. Qualitatively similar behavior in the early and middle stages of coalescence were observed in a thick cell, $h = 19\,\mu\text{m}$ [Figs. 4(a) and 4(b)]. Two regimes with power-law dependence of W from time [Fig. 4(b)] were found. However, at the middle stage of coalescence the exponent $\beta \approx 1/5$ [Fig. 4(b)]. As to the final stage, for droplets of large size $R > 30\,\mu\text{m}$ the relaxation of the ellipse to a circle is hindered. This did not allow one to conduct measurements in thick cells on droplets of large size ($R/h > 1.5$).

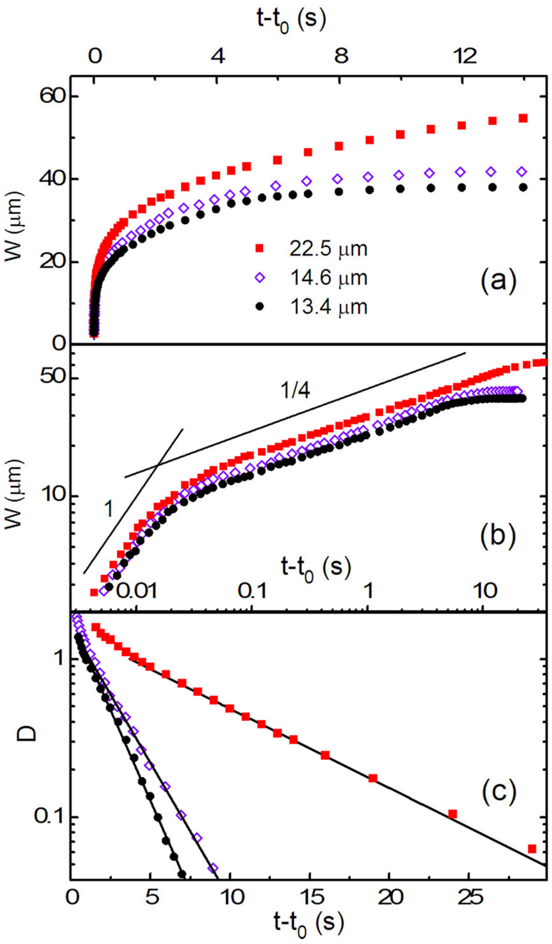

FIG. 3. The width of droplet bridge W versus time for isotropic droplet coalescence (a). Log-log (b) presentation of the experimental dependence of W on time. (c) Log-time representation of the shape factor $D = (L/W - 1)$ at droplet relaxation to circular form. The radii of initial droplets are $R_1 \approx 22.5\,\mu\text{m}$, $R_2 \approx 14.6\,\mu\text{m}$, and $R_3 \approx 13.4\,\mu\text{m}$. Thickness of the cell is $h = 5.5\,\mu\text{m}$.

Figure 5 compares the coalescence of droplets of approximately the same size ($R = 22.2\,\mu\text{m}$ and $R = 22.5\,\mu\text{m}$) in cells of different thickness. In the first regime, at the start of coalescence the linear behavior of bridge growth is observed with approximately the same velocity. The duration of the linear regime is greater in the thick cell. The crossover from the first to the second regime in the thick cell takes place at larger W. After the first crossover the velocity of the bridge growth decreases. It can be noted that the slope of log-log dependence after the first crossover is somewhat smaller in the thick cell than in the thin one [Fig. 5(b)]. After the second crossover the droplet relaxes in an exponential manner to its equilibrium circular form [Fig. 5(c)]. The moment of the second crossover also depends on cell thickness. Contrary to the first crossover, in the thicker cell it takes place at an earlier time. The slope of dependence of ln$D$ on time is larger in the thicker cell [Fig. 5(c)]. So, thick quasi-two-dimensional droplets transform to equilibrium form faster than thin droplets. Meanwhile, in the cell of the same thickness (Fig. 3 or Fig. 4) small droplets relax to equilibrium form faster. Both these effects are due to surface resistance (decrease of the velocity of the flow near the surface).

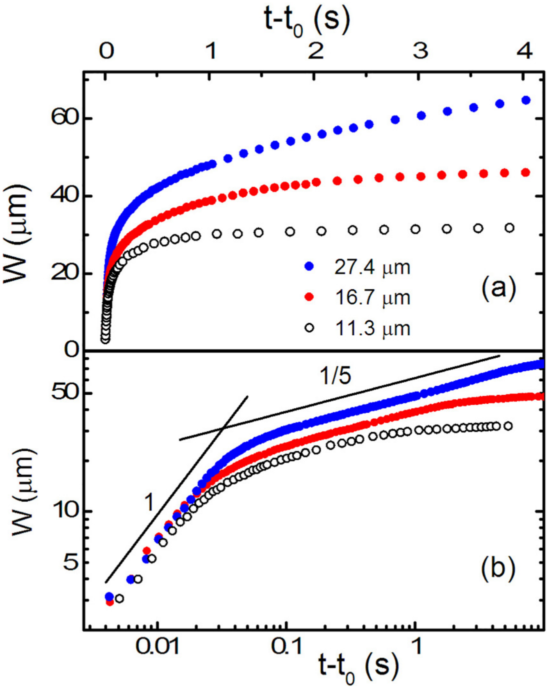

FIG. 4. Linear (a) and log-log (b) representation of the experimental dependence of W on time in a thick cell with $h = 19\,\mu\text{m}$. The radii of initial droplets R are about 27.4, 16.7, and 11.3 μm.

In our experiments the droplets were brought into contact to induce coalescence by slow heating of the sample so that the droplet radius slowly increased. The heating rate was typically 0.05 °C/ min. The question could arise whether some of the observed effects might be related to heating. We performed some measurements with different heating rates (0.05 °C/ min and 0.2 °C/ min) in thin and thick cells and on droplets of close sizes (Fig. 6). We see that the behavior at all three stages of coalescence is identical and the crossovers between regimes occur at the same times. At relatively small rates heating initiates droplet coalescence but does not influence its process.

IV. DISCUSSION

Coalescence dynamics is determined by the balance between the forces leading to coalescence and the resistance due to viscous and inertial forces. The most studied situations were the two limiting cases when the outer fluid medium is absent or when the viscosity of the inner medium can be neglected with respect to the outer medium. These two cases correspond to the coalescence of liquid droplets in air and the coalescence of bubbles in liquid [4,24]. The first theory of viscous two-dimensional coalescence was developed by Hopper [16]. He calculated the time evolution of the shape of two coalescing cylinders of equal size. The plane flow perpendicular to the cylinder axis was considered. So, this case corresponds to two-dimensional coalescence. The starting state in the calculations was an inverted ellipse (i.e., a figure obtained by inversion of an ellipse with respect to a unit circle) arbitrarily

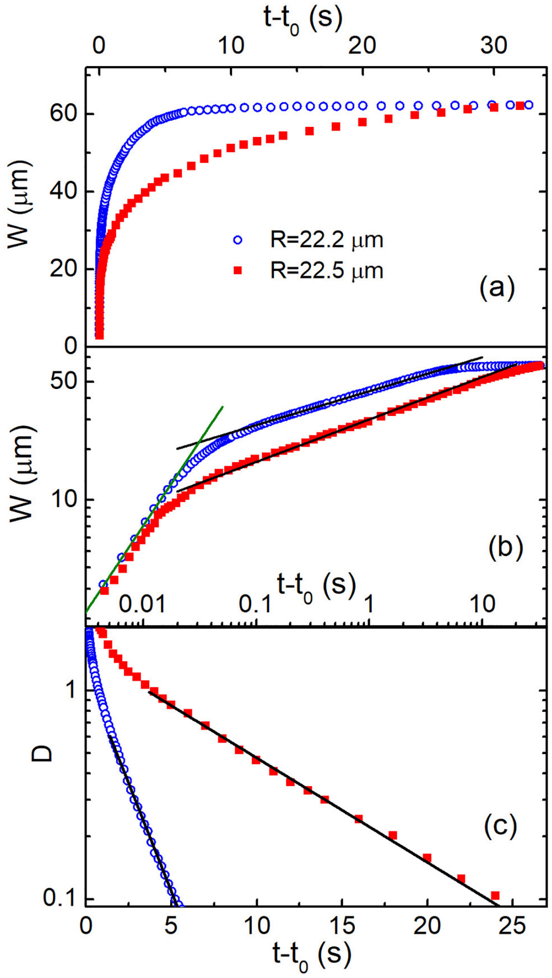

FIG. 5. The time evolution of the bridge width W for droplets with approximately the same radius but different cell thickness. Blue open circles: $R \approx 22.2$ μm, $h = 19$ μm; red closed squares: $R \approx 22.5$ μm, $h = 5.5$ μm. (a),(b) Dependence of W on time in linear and log-log representation; (c) log-time representation of the shape factor $D = (L/W - 1)$. The solid lines in (c) are exponential functions.

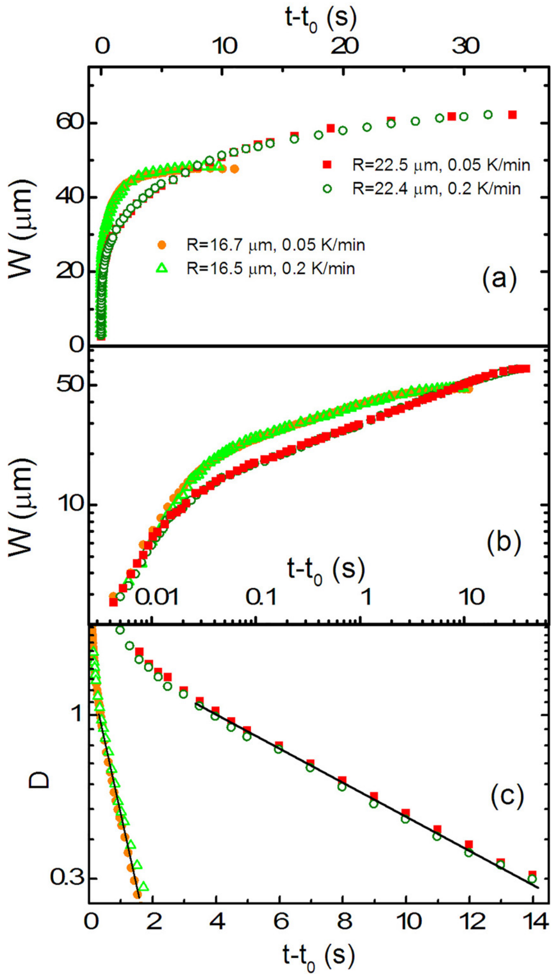

FIG. 6. The time dependence of bridge width W (a),(b) and shape factor $D = (L/W - 1)$ in (c) depend on droplet radius R and cell thickness h but do not depend on heating rate (0.05 °C/ min, solid symbols and 0.2 °C/ min, open symbols). Red closed squares, green open circles: $h = 5.5$ μm. Orange closed circles, green open triangles: $h = 19$ μm.

close to two tangent circles. Hopper has shown [16] that its evolution takes place through a sequence of inverted ellipses up to the final state, which is a circle. In Hopper's theory at the early stage of the coalescence the bridge between two droplets is very small and rapidly increases during droplet evolution. At the middle stage the inverted ellipse has a waist form as in experiments. At longer time it relaxes to a circle. Hopper's equations qualitatively describe the experimental data on the two-dimensional coalescence of islands in freestanding films [8,9,11].

The theory of three-dimensional coalescence predicts the existence of several coalescence regimes [4,24]. For droplets in the absence of external fluid at the initial stage of coalescence the bridge width grows in a linear manner with time, according to the so-called inertially limited viscous regime [4,24]. When the influence of the inner fluid can be neglected and the dynamics is governed by the outer medium, the bridge should grow as the square root of time [4]. A transition between different regimes can be observed with a change of the relative viscosity and density of the inner and the outer fluid or in the process of coalescence with an increase of the bridge size. The relative influence of viscous and inertial forces on dynamics is described by the dimensionless Ohnesorge number $\mathrm{Oh} = \mu/\sqrt{\rho\gamma r_S}$, where μ is the dynamical viscosity, ρ is the fluid density, γ the interface tension, and r_S is the characteristic size [4,20]. A large Ohnesorge number corresponds to a viscous regime. In our case when the viscosities of the droplet and the environment are close, we consider μ as the sum of the viscosities of droplet μ_1 and environment μ_2 (isotropic liquid and nematic). The densities of both phases are about 1 g/cm^3 [35]. The viscosity of the nematic phase is anisotropic. At homeotropic alignment the viscosity of nematic is close to Miesowicz viscosity η_c [27]. The viscosities of the isotropic phase and nematic close to the isotropic-nematic transition determined by Oswald and Poy in a similar compound 7CB [27] are about 2.35×10^{-2} and 3.52×10^{-2} Pa s. The value of the nematic-isotropic interface tension in 7CB is 1.12×10^{-5} N/m [27]. As the effective size r_S one can take the width of the droplet bridge W, which is in the range of about 3–80 μm (Figs. 3–6). Using these parameters, we find that the Ohnesorge number in our case varies from approximately 62 to 320. So, our conditions correspond to the viscous regime. Large values of a Ohnesorge number are in part due to the small value of the nematic-isotropic interface tension. The interface tension between two different liquids can be substantially larger, for example γ between droplets and environment in the experiments of Yokota and Okumura [30] was about 2×10^{-2} N/m.

In our case the situation is more complicated and richer with respect to three-dimensional coalescence due to the influence of confined geometry and dissipation related to the Poiseuille flow [27,30,37]. We found three distinct regimes of coalescence that change one to another with time (Figs. 3–5). The first and third regimes exist at the coalescence of both large and small droplets. The second regime exists in large droplets ($2R > h$). The width of the second regime decreases with the decrease of the droplet radii [Figs. 3(b) and 4(b)] and disappears at the coalescence of small droplets. Some of the listed regimes were observed in Hele-Shaw cells or in three-dimensional geometry. However, to the best of our knowledge, three sequential regimes following one after the other with different functional dependence were never investigated in any materials and geometries. It should be noted also that the geometry of experiment sometimes imposes restrictions on the final stage of coalescence, for example, in experiments on pendant droplets [2,3,24]. In such experiments usually it is possible to investigate only the early stage of coalescence when the size of the bridge does not exceed the initial droplet radius. In our study it is possible to follow the modification of the droplet shape from the start of coalescence until relaxation to the circular form.

Now we discuss in detail every observed coalescence regime.

A. Short-time regime

In the beginning of the coalescence we observed linear dependence of the bridge size W on time (Figs. 3–5). The rate of bridge growth is nearly the same for droplets of different size and cell thickness. The main transformation takes place near the contact point of two droplets when $2r \approx (W/2)^2/R$ (Fig. 2) is smaller than h. After the start of coalescence the material moves mostly in the meniscus of the droplets. We may guess that at this stage the cell surface and the Poiseuille flow do not play an essential role in coalescence dynamics and the situation is similar to the coalescence of free droplets. According to Hopper's theory [16] for two-dimensional coalescence the functional dependence of bridge expansion is linear with logarithmical correction. In the years following Hopper's work, both three-dimensional and quasi-two-dimensional coalescence were studied using different theories and numerical calculations [17–23]. Scaling theory was widely used for prediction and for explanation of the evolution of a bridge formed at droplet coalescence. According to a simple consideration for a viscous droplet at early time the scaled bridge width $W/2R$ is inversely proportional to scaling time $W/2R = A_1 t/\tau$, where $\tau = \mu R/\gamma$ [21,24]. So, the bridge width grows with capillary velocity $V_C = \gamma/\mu$ multiplied by a dimensionless coefficient A_1 of order of unity. Eggers *et al.* [18] obtained the early time asymptotical dependence for systems of different dimensionality $W/2R \sim A_1 t/\tau |\ln(t/\tau)|$, where coefficient A_1 contains a multiplier $(\alpha - 1)$ that depends on the dimensionality of the system α. At the coalescence of droplets in air μ stands for the viscosity of droplets, and at the coalescence of bubbles, for the viscosity of the environment.

In previous experiments [1,3,21,24] the expansion of the bridge with a nearly linear dependence on time was observed. So, our results about nearly linear dependence of W on time support the guess that at the early stage the coalescence of sandwiched droplets can be considered as free coalescence. A similar assumption was previously made by Yokota, Okumura [30,32], and Chinaud *et al.* [31] who investigated the merging of a flat droplet composed by a glycerol-water mixture with a bath of the same mixture. In their cell the single droplet was surrounded by low-viscosity oil and sandwiched between two glass plates with a large gap of about 1 mm. The time dependence of the bridge width W between droplet and bath was measured. The linear dependence of the bridge width at short time was found [30–33] that correlates with our observation for a different process, namely, coalescence of two droplets.

Referring to the dimensionless expression $W/2R \approx t/\tau$ the experimental data for W were scaled by $2R$ and time by τ so that the data at short time collapsed on the same line [Fig. 7(a)]. In such way we obtained the characteristic time τ [Fig. 8(a), closed circles for cell thickness 5.5 μm; open circles for cell thickness 19 μm]. For free coalescence the characteristic time τ depends on R in a linear manner and practically does not depend on cell thickness within the range of experimental error.

B. Middle-time regime

After the linear dependence in the short-time regime (Figs. 3–5) we did not find a transition to square root dependence which was observed in a number of experiments [3,4,21]. Instead, we observed a smoother dependence $W \sim t^{\beta}$ with β about 1/4 in the cell with gap 5.5 μm and about 1/5 in the thick cell with gap 19 μm (Figs. 3–5). Crossover times between the first and the second regime increase with thickness of the cell (Fig. 5) as expected for droplets with a larger meniscus. The transition to the second regime is related to confined geometry when dissipation connected with the Poiseuille flow (surface resistance) is dominant. Such dissipation was considered by Yokota and Okumura [30]. The velocity gradient results from Poiseuille flow between cell surfaces. So, dissipation related to gradient along the bridge (first stage) changes during the crossover to dissipation related to gradient perpendicular to the bridge (later stage). In the second regime the rate of change of the surface energy is estimated as $\gamma d(Wh)/dt$ and Poiseuille dissipation $\mu(V/h)^2 2Whr$ in volume $2Whr$, where $V \approx dW/dt$ and $2r \approx (W/2)^2/R$ (see Fig. 2). This consideration gives $W \propto (\gamma R h^2 t/\mu)^{1/4}$ similar to [30] or scaling $W/2\sqrt{Rh} = A_2 (t/\tau_s)^{1/4}$ with $\tau_s = (\mu/\gamma)R$ and with dimensionless constant A_2. This power dependence correlates with our data for thin cells (Fig. 3; $h = 5.5$ μm).

Keeping in mind that the power function $W \sim [(t - t_0)/\tau_s]^{\beta}$ with exponent $\beta = 1/4$ is in agreement with the theoretical dependence for merging of a droplet with a straight boundary, we scale the experimental data for the 5.5 μm cell varying τ_s and t_0 to obtain the universal

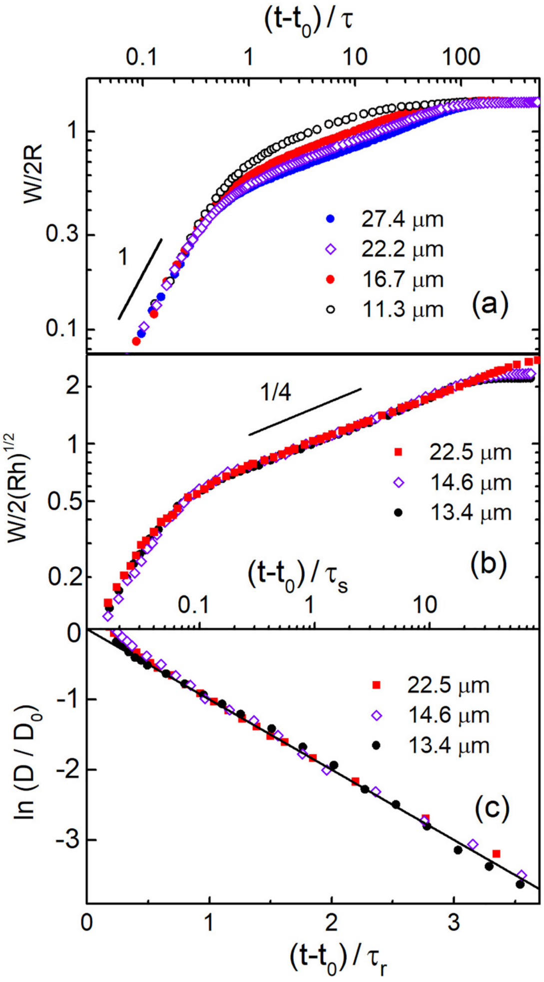

FIG. 7. Scaled experimental data demonstrating three different regimes. (a) The experimental dependence of scaled bridge width $W/2R$ on scaled time $(t - t_0)/\tau$ for droplets of different sizes that demonstrates linear dependence at the initial stage of coalescence. Thickness of the cell $h = 19\,\mu\text{m}$. (b) The dependence of $W/2\sqrt{Rh}$ on $(t - t_0)/\tau_s$. The data were scaled in the middle-time region, $h = 5.5\,\mu\text{m}$. (c) The dependence of scaled shape factor D/D_0 on $(t - t_0)/\tau_r$ shown for the late stage of coalescence. The solid line is the dependence $\ln(D/D_0) = -t/\tau_r$. $h = 5.5\,\mu\text{m}$.

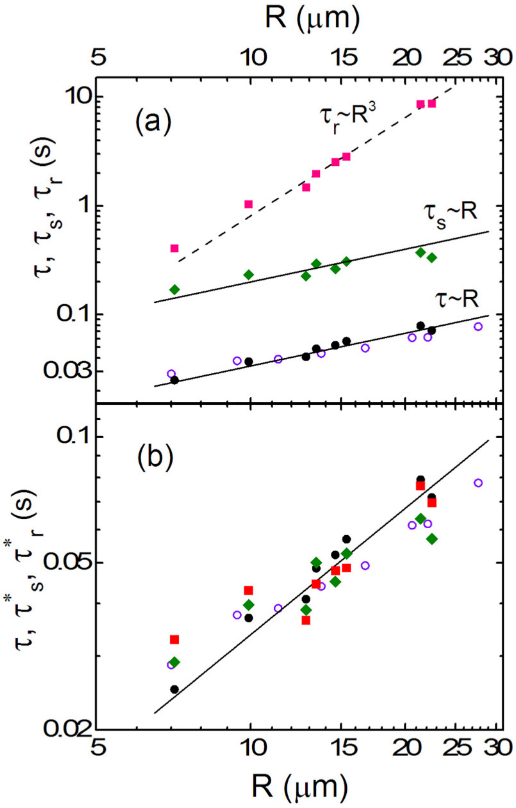

FIG. 8. (a) Characteristic times for different stages of coalescence and different film thickness. Circles, diamonds, and squares are characteristic times (τ, τ_s, and τ_r) for early, middle, and final stages of coalescence. Closed symbols: $h = 5.5\,\mu\text{m}$; open symbols: $h = 19\,\mu\text{m}$. Early-stage characteristic times τ are close in thin and thick samples. The characteristic times for the later stages are given for the thin cell ($h = 5.5\,\mu\text{m}$). The straight lines are guides to the eye; the solid lines have the slope 1, the dashed line corresponds to $\sim R^3$ dependence. (b) Characteristic times at the initial-stage τ (circles), rescaled middle-stage τ_s^*, and late-stage τ_r^* times rescaled to $R\mu/\gamma$ for the 5.5 μm cell (diamonds and squares).

dependence of $W/2\sqrt{Rh}$ on time scaled by τ_s. Here, we take $A_2 = 1$. For different droplet radii the experimental dependence $\ln(W/2\sqrt{Rh})$ collapsed onto the master curve by a suitable choice of τ_s [Fig. 7(b)]. Starting time t_0 was close to the value determined from the linear dependence at the initial stage. For the data in Fig. 7(b) the universal dependence with exponent $\beta = 1/4$ is observed over two decades of dimensionless time $(t - t_0)/\tau_s$. The characteristic times τ_s obtained in such a way are shown in Fig. 8(a) by diamonds. τ_s depend on R in a linear manner in accordance with the arguments given above. The dependence is the same as for the early-stage times τ, but the values of τ_s are about six times larger [Fig. 8(a)]. It should be noted that the numerical coefficient A_2 in the scaling relation is not known. If a different value of A_2 is taken instead of $A_2 = 1$, it is equivalent to multiplication of all the characteristic times by the same coefficient $(A_2)^4$ and it does not change the functional dependence of τ_s on R. In particular, we can take the value of A_2 such that the rescaled characteristic times τ_s^* [Fig. 8(b); diamonds] become close to the times at the early stage τ. The values of τ_s^* in Fig. 8(b) correspond to $A_2 \approx 0.64$. We may guess that our results allow estimating the numerical coefficient A_2. It was possible because we observed several regimes of coalescence in a single event. Our value of A_2 can be compared to the results of Yokota and Okumura [30]. The value of A_2 estimated from the data [30] at the initial and middle stages of coalescence is also found to be of the order of unity, $A_2 \approx 1.2$. The difference with respect to our result ($A_2 \approx 0.64$) can be related, in particular, to different geometry of coalescence, namely, the coalescence of two circular droplets in our case and the coalescence of a circular droplet with a bath in [30]. Another possible reason is that in [30] the droplet is surrounded by a liquid of considerably smaller viscosity, and in our case the viscosity of the surrounding medium is comparable to the viscosity of the droplet.

As to our data for the 19 μm cell, we remind one that there is some difference in slope of $\ln(W)$ in the middle-time range with respect to thin cells (Figs. 3–5). Although the difference in slope is small, it is clearly reproduced in the measurements. Power-law dependence with exponent $\beta = 1/5$ has not been observed previously and now its origin is not clear. The reason could be that the ratios of R/h in the case of the 19 μm cell are relatively small, and the condition of quasi-two-dimensional geometry used to derive the functional dependence [30] is not fully applicable.

C. Final regime, relaxation to circular form

Relaxation dynamics of elliptical or ellipsoidal droplets [38], vesicles [39,40] to equilibrium circular or spherical shape is essential for fundamental sciences, technical applications, and biology. In previous experiments external forces (electric field, elongation flow) were applied to create a nonequlibrium droplet shape [39,40]. In our case a nearly elliptical droplet is formed on the final stage of droplet coalescence [Figs. 1(e) and 1(f)]. In theoretical works different starting shapes of the coalescing droplet were considered. In Hopper's theory [16] the droplet boundary is an inverse ellipse, which is represented by a bicircular curve of fourth degree, also called the lemniscate of Booth [41]. On the final stage of relaxation to circle the shape of the inverse ellipse is very close to ellipse. The transformation of the shape was described during the whole coalescence process by one relaxation time $\tau = \mu R/\gamma$ [16]. Exponential relaxation to circular form was observed for smectic islands in freestanding films [9] that can be considered as a quasi-two-dimensional system. In freestanding films and Hele-Shaw cells the physics of the driving force is the same, but in Hele-Shaw cells the resistance to droplet relaxation is related to Poiseuille flow. This does not change the functional (exponential) dependence of relaxation during the final stage, but essentially increases the relaxation time $\tau_r \propto BR^3\mu/h^2\gamma$, where B is a nondimensional constant $B \approx 2^{3/2}/0.38$ [27,37]. Brun *et al.* [37] and Oswald and Poy [27] have shown that in the limit of small distortion $D(t) = D(0)\exp(-t/\tau_r)$. The relaxation time can be written in our case as

$$\tau_r = BR^3(\mu_1 + \mu_2)/h^2\gamma. \tag{1}$$

Exponential relaxation is demonstrated in Fig. 7(c). Time is scaled by τ_r. Shape factor $D(t)$ is scaled by a suitable value D_0 so that the data at the late-stage collapse on the same curve $\ln(D/D_0) = -t/\tau_r$. Relaxation times τ_r determined from exponential dependence on the final stage of coalescence are shown by squares in Fig. 8(a). The values of τ_r are approximately proportional to R^3 in accordance with (1). We can compare the relaxation dynamics with the characteristic time at the early stage of coalescence. Based on the theoretical expression (1) we scale our values τ_r found from experiment by multiplying them by h^2/BR^2 so that the expression for the characteristic time coincides with the equation $\tau = \mu R/\gamma$. The rescaled relaxation times τ_r^* are shown in Fig. 8(b) by red squares. It is remarkable that the rescaled values fall in the same range as the times for the initial stage. For the thick cells we do not analyze the data at the relaxation stage, since the range of values $R/h < 1.5$ for our measurements in the 19 μm cell is smaller than the range of ratios R/h of the quasi-two-dimensional geometry considered in [27,37]. To analyze the results for $R/h < 1.5$ quantitatively, a theory has to be developed.

From the dependence of characteristic times on R we can estimate the capillary velocity γ/μ which governs the coalescence dynamics. At the initial stage of coalescence, the bridge width grows linearly with time with approximately the same rate in thick and thin cells. The solid line in Figs. 8(a) and 8(b) corresponds to ratio $\tau/R = 3.38 \times 10^{-3}$ s/μm. The dependence of the bridge width at the initial stage is given by $W/2R = (t/\tau) = (\gamma/\mu R)t$, so we get $\gamma/\mu = (\tau/R)^{-1} \approx 3 \times 10^{-4}$ m/s. Taking for comparison the values of γ and μ determined by Oswald and Poy [27], we get the value of capillary velocity about 2×10^{-4} m/s. Note that if we take the value of interface tension between the isotropic and nematic phases 1.8×10^{-5} N/m as determined by Faetti and Palleschi [42], the capillary velocity is about 3.1×10^{-4} m/s, which is very close to our value.

V. SUMMARY

About 40 years ago, Hopper in his seminal work [16] investigated two-dimensional coalescence of two viscous cylinders. The obtained analytical expressions described structure transformation on different stages of coalescence using one characteristic time $\tau = R\mu/\gamma$. Since then, experimental and theoretical studies of two-dimensional and three-dimensional coalescence of droplets and bubbles have shown that the situation can be essentially complicated. Several coalescence regimes were found (inertial, viscous, and intermediates) that can be observed at the same coalescence event. Then, it was shown that confined geometry and Poiseuille flow open additional possibilities for coalescence dynamics. In our paper we describe in details the structure features of coalescence in Hele-Shaw cells on different stages of coalescence. Time dependence of the bridge width and droplet shape factor was experimentally determined for droplets of different size in cells of different thickness. Experimental results are discussed on the basis of existing theoretical models. In the beginning of coalescence, the rate of bridge growth does not depend on droplet radius and cell thickness. In the middle and final stages, the coalescence dynamics is determined by Poiseuille flow. For thin cells, characteristic times $\tau = R\mu/\gamma$ obtained from initial, middle, and relaxation stages of coalescence can be collapsed on the same dependence on R. Late-stage relaxation is faster in thicker cells.

Several aspects can be explored in further investigations. In particular, it is tempting to study the crossover from quasi-two-dimensional to three-dimensional coalescence of droplets and clarify the origin of the difference in power-law exponent at the intermediate stage in thin and thick cells. These would be subjects of future studies.

The authors declare no conflict of interest.

ACKNOWLEDGMENT

The reported study was supported by Russian Science Foundation Grant No. 23-12-00200.

[1] D. G. A. L. Aarts, H. N. W. Lekkerkerker, H. Guo, G. H. Wegdam, and D. Bonn, Hydrodynamics of droplet coalescence, Phys. Rev. Lett. **95**, 164503 (2005).

[2] S. C. Case and S. R. Nagel, Coalescence in low-viscosity liquids, Phys. Rev. Lett. **100**, 084503 (2008).

[3] J. D. Paulsen, J. C. Burton, and S. R. Nagel, Viscous to inertial crossover in liquid drop coalescence, Phys. Rev. Lett. **106**, 114501 (2011).

[4] J. D. Paulsen, R. Carmigniani, A. Kannan, J. C. Burton, and S. R. Nagel, Coalescence of bubbles and drops in an outer fluid, Nat. Commun. **5**, 3182 (2014).

[5] C. R. Anthony, M. T. Harris, and O. A. Basaran, Initial regime of drop coalescence, Phys. Rev. Fluids **5**, 033608 (2020).

[6] M. Heinen, M. Hoffmann, F. Diewald, S. Seckler, K. Langenbach, and J. Vrabec, Droplet coalescence by molecular dynamics and phase-field modeling, Phys. Fluids **34**, 042006 (2022).

[7] D. H. Nguyen, Smectic liquid crystal freely suspended films: Testing beds for the physics in thin membranes, Ph.D. thesis, University of Colorado Boulder, 2011, https://scholar.colorado.edu/phys_gradetds/41.

[8] R. Stannarius and K. Harth, Inclusions in freely suspended smectic films, in *Liquid Crystals with Nano and Microparticles*, edited by J. P. F. Lagerwal and G. Scalia (World Scientific, Singapore, 2017), pp. 401–405.

[9] N. S. Shuravin, P. V. Dolganov, and V. K. Dolganov, Coalescence of viscous two-dimensional smectic islands, Phys. Rev. E **99**, 062702 (2019).

[10] P. V. Dolganov, N. S. Shuravin, E. I. Kats, and V. K. Dolganov, Coalescence of islands of different thicknesses in smectic nanofilms, JETP Lett. **110**, 545 (2019).

[11] Z. H. Nguyen, K. Harth, A. M. Goldfain, C. S. Park, J. E. Maclennan, M. A. Glaser, and N. A. Clark, Coalescence of islands in freely suspended smectic films, Phys. Rev. Res. **3**, 033143 (2021).

[12] P. V. Dolganov, N. S. Shuravin, and V. K. Dolganov, Coalescence of holes in two-dimensional free-standing smectic films, Phys. Rev. E **101**, 052701 (2020).

[13] P. V. Dolganov, N. S. Shuravin, V. K. Dolganov, and E. I. Kats, Dynamics of island-meniscus coalescence in free-standing smectic films, Soft Matter **16**, 8506 (2020).

[14] C. Klopp, T. Tritel, and R. Stannarius, Self similarity of liquid droplet coalescence in a quasi-2D free-standing liquid-crystal film, Soft Matter **16**, 4607 (2020).

[15] C. Klopp and A. Eremin, On droplet coalescence in quasi-two-dimensional fluids, Langmuir **36**, 10615 (2020).

[16] R. W. Hopper, Coalescence of two equal cylinders: Exact results for creeping viscous plane flow driven by capillarity, J. Am. Ceram. Soc. (Commun.) **67**, C-262 (1984).

[17] R. E. Goldstein, A. I. Pesci, and M. J. Shelley, Topology transitions and singularities in viscous flows, Phys. Rev. Lett. **70**, 3043 (1993).

[18] J. Eggers, J. R. Lister, and H. A. Stone, Coalescence of liquid drops, J. Fluid Mech. **401**, 293 (1999).

[19] Y. Lee and J. E. Sprittles, Capillary breakup of a liquid bridge: Identifying regimes and transitions, J. Fluid Mech. **797**, 29 (2016).

[20] X. Xia, C. He, and P. Zhang, Universality in the viscous-to-inertial coalescence of liquid droplets, Proc. Natl Acad. Sci. USA **116**, 23467 (2019).

[21] M. Rahman, W. Lee, A. Iyer, and S. J. Williams, Viscous resistance in drop coalescence, Phys. Fluids **31**, 012104 (2019).

[22] S. Perumanath, M. K. Borg, M. V. Chubynsky, J. E. Sprittles, and J. M. Reese, Droplet coalescence is initiated by thermal motion, Phys. Rev. Lett. **122**, 104501 (2019).

[23] D. Beloborodov and A. Vishnyakov, Molecular dynamics of nanodroplet coalescence in quasi-saturated vapor, Fluids **8**, 77 (2023).

[24] J. D. Paulsen, J. C. Burton, S. R. Nagel, S. Appathural, M. T. Harris, and O. A. Basaran, The inexorable resistance of inertia determines the initial regime of drop coalescence, Proc. Natl Acad. Sci. USA **109**, 6857 (2012).

[25] J. D. Paulsen, Approach and coalescence of liquid drops in air, Phys. Rev. E **88**, 063010 (2013).

[26] P. Pieranski, L. Beliard, J.-Ph. Tourellec, X. Leoncini, C. Furtlehner, H. Dumoulin, E. Riou, B. Jouvin, J. P. Fénerol, Ph. Palaric, J. Hueving, B. Cartier, and I. Kraus, Physics of smectic membranes, Physica A (Amsterdam, Neth.) **194**, 364 (1993).

[27] P. Oswald and G. Poy, Droplet relaxation in Hele-Shaw geometry: Application to the measurement of the nematic-isotropic surface tension, Phys. Rev. E **92**, 062512 (2015).

[28] P. V. Dolganov, A. S. Zverev, K. D. Baklanova, and V. K. Dolganov, Dynamics of capillary coalescence and breakup: Quasi-two-dimensional nematic and isotropic droplets, Phys. Rev. E **104**, 014702 (2021).

[29] P. V. Dolganov, A. S. Zverev, K. D. Baklanova, and V. K. Dolganov, Quasi-two-dimensional coalescence of nematic and isotropic droplets and Rayleigh-Plateau instability in flat optical cells, Soft Matter **18**, 126 (2022).

[30] M. Yokota and Ko Okumura, Dimensional crossover in the coalescence dynamics of viscous drops confined in between two plates, Proc. Natl. Acad. Sci. USA **108**, 6395 (2011).

[31] M. Chinaud, V. Voulgaropoulos, and P. Angeli, Surfactant effects on the coalescence of a drop in a Hele-Shaw cell, Phys. Rev. E **94**, 033101 (2016).

[32] Ko Okumura, Viscous dynamics of drops and bubbles in Hele-Shaw cells: Drainage, drag friction, coalescence, and bursting, Adv. Colloid Interface Sci. **255**, 64 (2018).

[33] Y. M. Koga and Ko Okumura, Inertial coalescence of a liquid drop surrounded by viscous liquid, J. Phys. Soc. Jpn. **91**, 025001 (2022).

[34] H. Wang, T. X. Wu, S. Gauza, J. R. Wu, and S.-T. Wu, A method to estimate the Leslie coefficients of liquid crystals based on MBBA data, Liq. Cryst. **33**, 91 (2006).

[35] F. A. de Sousa, R. N. Michels, P. M. M. Cardoso, and M. M. A. de Jesus, Experimental proof of an anomalous behavior in the nematic phase of the liquid crystal E7, Mol. Cryst. Liq. Cryst. **576**, 106 (2013).

[36] R. Basu, D. Kinnamon, N. Skaggs, and J. Womack, Faster in-plane switching and reduced rotational viscosity characteristics in a graphene-nematic suspension, J. Appl. Phys. **119**, 185107 (2016).

[37] P.-T. Brun, M. Nagel, and F. Gallaire, Generic path for droplets relaxation in microfuidic channels, Phys. Rev. E **88**, 043009 (2013).

[38] S. Guido and M. Villone, Measurement of interfacial tension by drop retraction analysis, J. Colloid Interface Sci. **209**, 247 (1999).

[39] R. Dimova, K. A. Riske, S. Aranda, N. Bezlyepkina, R. L. Knorr, and R. Lipowsky, Giant vesicles in electric fields, Soft Matter **3**, 817 (2007).

[40] M. Yu, R. B. Lira, K. A. Riske, R. Dimova, and H. Lin, Ellipsoidal relaxation of deformed vesicles, Phys. Rev. Lett. **115**, 128303 (2015).

[41] I. S. Sokolnikoff, *Mathematical Theory of Elasticity*, 2nd ed. (McGraw-Hill, New York, 1956), pp. 157–159, 249–312 (Sec. 45, 65–86).

[42] S. Faetti and V. Palleschi, Measurement of the interfacial tension between nematic and isotropic phase of some cyanobiphenyls, J. Chem. Phys. **81**, 6254 (1984).